J. Inst. Eng. India Ser. D
https://doi.org/10.1007/s40033-026-01017-w

ORIGINAL CONTRIBUTION

Experimental and Thermo-Statistical Optimization of Tool Geometry and Process Parameters in Friction Stir Welding of AA3103 Aluminium Alloy

Ganesh Jagannath Pagar[1,2] · Gajanan N. Shelke[3]

Received: 14 January 2026 / Accepted: 12 April 2026

Abstract This study investigates the combined influence of tool pin geometry, shoulder-to-pin diameter ratio (D/d), spindle speed, and welding speed on material flow, temperature distribution, and surface quality during friction stir welding (FSW) of AA3103 aluminium alloy. A Taguchi L9 orthogonal array was employed to minimize experimental trials while identifying the most significant process factors. Twenty-seven welds were fabricated using three distinct tool pin profiles square, circular, and triangular and evaluated through infrared thermography and surface profilometry. The results revealed that higher spindle speeds coupled with lower welding speeds enhanced material plasticization, reduced surface roughness, and improved heat uniformity across the weld zone. Among all configurations, the circular pin produced the most stable and defect-free welds, while square pins generated higher frictional heat but exhibited greater roughness variations. The optimum parameter combination of 710 RPM spindle speed, 20 mm/min traverse speed, and D/d = 4 achieved the lowest surface roughness (Ra ≈ 1.37 μm). Statistical and thermal correlation analyses confirmed that spindle speed was the dominant parameter influencing both heat input and surface morphology. The study establishes a novel thermo-statistical optimization framework for AA3103, integrating Taguchi-based design with infrared thermographic validation. The findings provide practical guidelines for achieving superior weld quality in lightweight aluminium applications across automotive and aerospace sectors.

Keywords Friction stir welding (FSW) · AA3103 aluminium alloy · Tool pin profile · Surface roughness · Taguchi method · Temperature distribution

Abbreviations

AA	Aluminium alloy
AA3103	Aluminium alloy 3103, Al–Mn series
FSW	Friction stir welding
DOE	Design of experiments
D/d	Shoulder-to-pin diameter ratio
D	Shoulder diameter of tool (mm)
d	Pin diameter of tool (mm)
N	Spindle rotational speed (RPM)
V	Welding or traverse speed (mm/min)
Ra	Arithmetic average surface roughness (μm)
T	Temperature (°C)
ρ	Density of material (kg/m^3)
Cp	Specific heat capacity (J/kg·K)
k	Thermal conductivity (W/m·K)
τ	Shear stress at tool–workpiece interface (MPa)
r_s	Radius of tool shoulder (mm)
r_p	Radius of tool pin (mm)
Q	Total frictional heat input (J or W)
Q_s	Heat generated by tool shoulder (J or W)
Q_p	Heat generated by tool pin (J or W)
ω	Angular speed of tool (rad/s)
v	Traverse velocity of tool (mm/s)
Pe	Peclet number, ratio of advection to diffusion

✉ Ganesh Jagannath Pagar
ganeshpagar25@gmail.com

Gajanan N. Shelke
gnshelke@gmail.com

[1] Department of Mechanical Engineering, MET's Institute of Engineering, (Savitribai Phule Pune University, Pune), Bhujbal Knowledge City, Nashik, Maharashtra, India

[2] SNJB's Shri Hiralal Hastimal (Jain Brothers, Jalgaon), Polytechnic, Chandwad, Nashik, Maharashtra, India

[3] Department of Mechanical Engineering, Sandip Foundation's, SIEM, Nashik, Maharashtra, India

Published online: 18 April 2026

t	Time (s)
x	Distance along weld line (mm)
T_{max}	Peak temperature in weld zone (°C)
μ	Coefficient of friction
σ	Standard deviation
S/N Ratio	Signal-to-noise ratio used in Taguchi analysis (dB)
ANOVA	Analysis of variance
KDE	Kernel density estimation used for surface roughness distribution
HMT FN2	Hindustan machine tools FN2 vertical milling machine
PWHT	Post weld heat treatment
P	Power input during friction stir welding (W)
T(x, t)	Temperature field as a function of distance and time (°C)
η	Process efficiency factor
f_s, f_p	Friction coefficients for shoulder and pin

Introduction

Friction Stir Welding (FSW), pioneered by The Welding Institute (TWI) in 1991, has emerged as a highly reliable solid-state joining technique, particularly well suited for aluminium and its alloys, due to its ability to produce defect-free joints with superior mechanical properties while avoiding melting-related issues. In contrast to conventional fusion-based welding processes, which involve melting and resolidification of the base material, FSW operates below the melting temperature and forms joints through intense frictional heating and severe plastic deformation. This unique joining mechanism fundamentally alters the metallurgical evolution of the weld zone, enabling the formation of fine-grained microstructures while avoiding common fusion-related defects such as porosity, solidification cracking, excessive distortion, and residual stress accumulation [1, 2]. Owing to these advantages, FSW produces joints exhibiting enhanced mechanical performance, superior metallurgical stability, and improved service reliability. The inherent energy efficiency and environmental sustainability of FSW further contribute to its growing industrial acceptance. The absence of filler materials, shielding gases, and post-weld heat treatments makes the process economically attractive and environmentally benign. These benefits have led to widespread adoption of FSW in critical applications across aerospace, automotive, marine, railway, and structural engineering sectors, where high joint integrity and dimensional stability are paramount [3, 4]. Despite its industrial maturity, the complex thermo-mechanical nature of FSW necessitates continuous research into process parameter optimization and tool design to ensure consistent weld quality across different aluminium alloy systems.

A considerable body of research has focused on clarifying how friction stir welding parameters affect heat input, material transport, and the resulting mechanical performance of welded joints. It has been established that factors including tool rotation rate, traverse speed, axial load, and tool design strongly control the thermal history and plastic deformation during the process. Investigations on AA5754-H24 have further shown that small changes in pin eccentricity and welding speed can markedly alter material flow characteristics and promote variations in grain refinement within the stir zone [3, 5]. These findings underscore the sensitivity of the FSW process to tool-workpiece interaction and highlight the need for precise control of geometrical parameters. Similarly, the shoulder-to-pin diameter ratio (D/d) has been identified as a critical factor influencing heat input and weld integrity. Investigations on AA7075-T651 joints demonstrated that an optimum D/d ratio improves thermal stability, enhances material consolidation, and leads to superior tensile strength [6, 7]. Comprehensive reviews of FSW process parameters and tool design have consistently concluded that pin profile and shoulder geometry are the dominant contributors to heat generation, defect suppression, and surface quality [8, 9]. Collectively, these studies emphasize that achieving defect-free welds requires a systematic approach to tool design and process optimization rather than isolated parameter adjustments.

Among tool design parameters, the tool pin profile is widely recognized as one of the most influential factors controlling material stirring, heat distribution, and plastic flow during FSW [10]. Investigations into AA6061-T6 have shown that circular and tapered pin profiles generally produce smoother surface finishes due to uniform material flow, whereas non-cylindrical profiles such as square or threaded pins enhance mechanical mixing but may introduce surface irregularities if not properly optimized [11, 12]. Advanced surface imaging studies further confirmed that tool geometry has a pronounced effect on surface roughness, defect density, and overall weld appearance [13, 14]. While these insights are well established for heat-treatable aluminium alloys belonging to the AA6xxx and AA7xxx series, limited attention has been directed toward Al–Mn series alloys such as AA3103, which exhibit distinct thermal conductivity and deformation characteristics during FSW.

Parallel to experimental investigations, statistical optimization techniques have gained prominence as effective tools for systematically improving weld quality. Approaches including Taguchi experimental design, response surface methodology (RSM), and grey relational analysis allow the systematic assessment of several process parameters while significantly limiting the number of required experimental trials. Taguchi–VIKOR hybrid optimization applied to AA5083 joints resulted in significant improvements in tensile strength and surface finish [15, 16]. Similarly,

Taguchi–grey relational analysis performed on AA6061-T6 identified tool rotational speed and welding speed as the most critical parameters influencing multiple performance responses simultaneously [17, 18]. Despite these advancements, most optimization studies have focused primarily on mechanical properties, with limited integration of thermal behaviour and surface morphology within a unified statistical framework.

The importance of thermal control in FSW has been further reinforced by recent developments in process monitoring and data-driven modeling. Investigations on multi-pin FSW of AA7020 demonstrated that heat input directly governs weld soundness, microstructural uniformity, and surface appearance [19–21]. Infrared thermography and real-time temperature monitoring have proven effective in correlating thermal response with weld quality, offering valuable insights into process stability. However, a significant research gap remains in understanding the combined effects of tool geometry, process parameters, and shoulder-to-pin diameter ratio on both temperature distribution and surface characteristics, particularly for non-heat-treatable alloys such as AA3103 [22]. AA3103 aluminium alloy is widely employed in heat exchangers, roofing sheets, chemical processing equipment, and lightweight structural components due to its excellent corrosion resistance, formability, and moderate strength. For such applications, surface finish and thermal stability are critical, as surface irregularities can adversely affect corrosion resistance and aesthetic performance. Therefore, achieving an optimal balance between heat generation and surface morphology during FSW is essential for extending the industrial applicability of AA3103 alloys [23–25].

To address the identified research gap, the present study conducts a comprehensive Taguchi-based experimental investigation on the friction stir welding of AA3103 aluminium alloy. The study integrates infrared thermography, surface profilometry, and statistical optimization to establish a thermo-statistical framework capable of correlating heat generation with surface morphology [26, 27]. By systematically analyzing the influence of tool geometry, process parameters, and D/d ratio, this work aims to provide deeper insights into parameter interactions specific to AA3103. The outcomes of this research are expected to offer practical guidelines for achieving defect-free, thermally stable, and aesthetically refined welds, thereby supporting the broader adoption of FSW in lightweight structural and automotive applications.

Experimental Design and Methodology

A Taguchi L9 orthogonal array was applied in three separate experimental runs to efficiently analyze the influence of multiple process parameters while keeping the number of trials to a minimum. This statistical design reduces resource consumption and enables robust analysis of variable interactions affecting weld quality. Experiments were performed on a vertical milling machine adapted for FSW, equipped with adjustable spindle speed and semi-automatic traverse control. AA3103 plates were securely clamped to prevent misalignment or vibration during welding. Three different tool geometries, namely square, circular, and triangular, were evaluated under a range of operating conditions. A total of 27 experiments were carried out, with nine trials assigned to each tool geometry according to an L9 orthogonal array. The investigation concentrated on three primary performance measures: heat generation, material flow characteristics, and surface quality. Heat distribution was monitored using infrared thermography, material flow was examined through visual observation, and surface finish was measured using a surface profilometer. By combining statistical design with hands-on experimentation, the study provides a clear understanding of how process parameters influence weld performance and helps identify suitable parameter combinations for achieving improved weld quality in AA3103 alloy.

Configuration Set-Up for Experimental Work

The FSW Operation setup is shown in Fig. 1. Welding trials were performed on a modified HMT FN2 vertical milling machine, with manual feed control used to regulate traverse speed precisely. AA3103 aluminium plates were securely clamped using a custom fixture to maintain consistent tool engagement and alignment. The Taguchi L9 orthogonal array was employed to evaluate the effects of tool pin geometry (square, circular, triangular), spindle speed (355, 710, 1400 RPM), welding speed (20, 40, 80 mm/min), and D/d ratios (3, 4, 5), resulting in 27 total runs. Infrared thermography monitored weld-zone temperatures during FSW, while a Mitutoyo SJ-210 profilometer measured surface roughness post-weld. This setup enabled correlation of tool design and process conditions with weld quality and thermal behavior.

The FN2 vertical milling machine, built from high-strength mild steel, was used for FSW trials due to its mechanical stability and cost-effectiveness, especially in research and educational settings is represented in Table 1. Originally intended for milling tasks like drilling and slotting, it was adapted for solid-state welding applications. While the FN2 offers automated spindle control, feed rate and positioning are manual, providing greater operator control. Operating on 220 V, its compact size (1520 × 310 mm) and large clamping area (1350 × 310 mm) support heavy-duty FSW setups, handling loads up to 350 kg safely. Manufactured by HMT, the machine blends reliability, precision,

(a) Milling machine

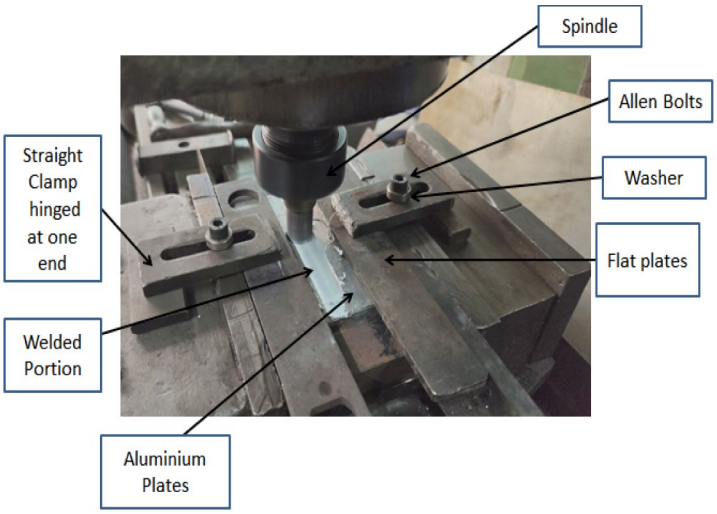

(b) Set-up for FSW Operation

Fig. 1 Experimental set-up

Table 1 Specifications of milling machine

Material	Mild steel
Product Type	FN2
Usage/Application	Milling
Automation Grade	Semi-Automatic
Voltage	220 V
Power Source	Electric
Weight	222 kg
Overall Dimensions (LxW)	1520×310 mm
Clamping Area (LxW)	1350×310 mm
Max. Safe Weight On Table	350 kg
Brand	HMT

and flexibility ideal for both academic and light industrial welding research.

Design of Experiment (DOE)

The Table 2 represents the study employed a 3 times Taguchi L9 orthogonal array to evaluate the influence of process parameters on the quality of friction stir welded (FSW) joints in AA3103 aluminium alloy. The Taguchi approach was adopted to conduct the study in a structured and efficient manner, limiting the total number of experiments to 27 while still maintaining reliable statistical evaluation. This method allowed the input parameters to be varied systematically and their individual effects to be examined without requiring an excessive number of trials. Three different tool pin shapes, square, circular, and triangular, were investigated. For each geometry, nine distinct parameter combinations were applied. The selected process variables included spindle speeds of 355, 710, and 1400 rpm, welding speeds of 20, 40, and 80 mm/min, and variations in the shoulder-to-pin diameter ratio (D/d). This experimental layout enabled a detailed study of the influence of each parameter, as well as their combined effects, on material flow behavior, heat generation, and surface quality.

The experimental trials were conducted on a vertical milling machine adapted for FSW. The AA3103 plates were clamped securely to ensure stable welding. During each run, infrared thermography was used to monitor temperature distribution, and a surface roughness tester evaluated the weld bead finish. These tools provided quantitative insights into weld consistency and quality. The process parameters were chosen because of their direct influence on heat input, plasticized material movement, and the overall soundness of the joint. For instance, increasing the spindle speed generally raises the heat generated during welding, but excessive speed may lead to overheating. On the other hand, reducing the welding speed increases the tool–material interaction time, which can improve material mixing, though it may also result in grain growth. The shoulder-to-pin diameter ratio (D/d) plays a significant role in determining the contact area and frictional heat generation, thereby affecting joint strength and surface appearance. In addition to conventional process parameters, tool pin geometry was treated as a major variable in this study. Variations in pin shape alter the stirring action and flow behavior of the softened material, offering deeper insight into the relationship between tool

Table 2 DOE as per Taguchi L9 Orthogonal Array for all three tool pin profile with parameters values

Sr. no	Parameters level design	Parameters values				
	D/d ratio	Speed of spindle (RPM)	Speed of weld (mm/min)	D/d ratio	Speed of spindle (RPM)	Speed of weld (mm/min)
For square tool						
1	1	1	1	15/5 = 3	355	20
2	1	2	2	15/5 = 3	710	40
3	1	3	3	15/5 = 3	1400	80
4	2	1	2	20/5 = 4	355	40
5	2	2	3	20/5 = 4	710	80
6	2	3	1	20/5 = 4	1400	20
7	3	1	3	25/5 = 5	355	80
8	3	2	1	25/5 = 5	710	20
9	3	3	2	25/5 = 5	1400	40
For circular tool						
10	1	1	1	15/5 = 3	355	20
11	1	2	2	15/5 = 3	710	40
12	1	3	3	15/5 = 3	1400	80
13	2	1	2	20/5 = 4	355	40
14	2	2	3	20/5 = 4	710	80
15	2	3	1	20/5 = 4	1400	20
16	3	1	3	25/5 = 5	355	80
17	3	2	1	25/5 = 5	710	20
18	3	3	2	25/5 = 5	1400	40
For triangular tool						
19	1	1	1	15/5 = 3	355	20
20	1	2	2	15/5 = 3	710	40
21	1	3	3	15/5 = 3	1400	80
22	2	1	2	20/5 = 4	355	40
23	2	2	3	20/5 = 4	710	80
24	2	3	1	20/5 = 4	1400	20
25	3	1	3	25/5 = 5	355	80
26	3	2	1	25/5 = 5	710	20
27	3	3	2	25/5 = 5	1400	40

design and weld performance. Square pins tend to create more intense stirring, circular pins promote smoother and more uniform flow, while triangular pins provide a moderate and balanced mixing effect. By combining the Taguchi design approach with systematic experimental trials, the study ensures efficient experimentation along with dependable results. This methodical framework helps in identifying suitable combinations of process and tool parameters, supporting the production of defect-free and mechanically sound welds in AA3103 alloy for industrial use.

Details of Selected Tools Profiles

The friction stir welding (FSW) trials were carried out using a vertical milling machine that was modified to enable FSW operations. AA3103 aluminium alloy plates were securely clamped on a fixed base using a custom fixture to prevent vibration or displacement. The tool spindle speed and traverse speed were controlled manually for precise parameter regulation during each trial. Figure 2 show the three tool pin profiles square, circular, and triangular were used, each machined from H13 tool steel. These profiles were selected to investigate their influence on material flow, heat generation, and weld bead characteristics under different process conditions.

Square Pin

Figure 2a represents the characterized by sharp edges, the square profile induces strong mechanical stirring and higher frictional heat, promoting deep penetration and refined grain structure. It is suitable for applications demanding high joint strength and structural integrity.

Circular Pin

Figure 2b shows the smooth, symmetrical shape, this profile ensures uniform heat distribution and stable material flow. It generates lower surface roughness and minimal defects, making it ideal for surface-sensitive applications.

Triangular Pin

Figure 2c represents the a hybrid design, the triangular profile introduces moderate turbulence and stirring. It balances heat input and material mixing efficiency, making it effective in scenarios requiring both structural performance and surface finish. These tools were evaluated across varying combinations of spindle speed, welding speed, and shoulder-to-pin diameter ratio to assess their overall impact on weld quality.

H13 tool steel, used for fabricating the FSW tools, offers high thermal resistance and mechanical strength, with a hardness of 48–52 HRC and a tensile strength of 1500 MPa. Its thermal conductivity (28 W/m·K) and operating temperature range (600–650 °C) make it suitable for high-heat applications like friction stir welding.

Result & Discussion

The evaluation of friction stir welding (FSW) experiments performed on AA3103 aluminium alloy, emphasizing the effect of principal process variables tool pin profile, spindle rotational speed, welding speed, and shoulder-to-pin diameter ratio (D/d) on weld integrity. Particular attention is given to their influence on material flow behaviour, thermal characteristics, and surface finish of the welds. A total of 27

(a) Square Pin Profile Tool

(b) Circular Pin Profile Tool

(c) Triangular Pin Profile Tool

Fig. 2 Actual tool images

experimental runs were methodically assessed to determine performance trends, interaction effects among parameters, and conditions conducive to producing sound, defect-free joints. Both individual and combined influences of the selected variables were examined to develop a comprehensive understanding of their contribution to weld quality. The results are discussed in subsequent subsections using visual observations, temperature measurements, and surface roughness evaluations, providing practical guidance for selecting appropriate FSW parameters.

Material Flow and Weld Observations

Material flow around the rotating tool is a critical aspect of the Friction Stir Welding (FSW) process, directly affecting joint consolidation, weld integrity, and surface finish. In this study, material flow behavior was assessed visually across 27 experimental trials, with observations shown in Fig. 3a–c for different tool profiles. Each tool pin geometry significantly influenced flow patterns. Tool pins with square and triangular profiles, characterized by flat faces and sharp edges, generated stronger stirring action and increased frictional heat. This enhanced the mixing of the softened material during welding. However, when combined with high shoulder-to-pin diameter ratios or excessive traverse speeds, these geometries sometimes led to defects such as flash formation, tunnel voids, or incomplete bonding due to irregular material movement. In comparison, the circular pin provided more consistent and uniform material flow under different processing conditions. Its smooth surface promoted steady heat generation and minimized surface irregularities, producing neater weld beads with fewer visible flaws. Spindle speed was another critical factor. At lower speeds, such as 355 RPM, the heat produced was often insufficient, resulting in inadequate plasticization and occasional discontinuities along the weld seam. Increasing the spindle speed improved material softening and facilitated smoother flow, provided the heat input was maintained within an appropriate range. Overall, the findings indicate that careful control of tool geometry, spindle speed, and the D/d ratio is essential to ensure proper material flow and produce sound, defect-free welds in AA3103 alloy. The circular pin is advantageous for thermal stability, while square pins offer aggressive stirring for strength-critical applications when process parameters are well optimized.

Temperature Distribution

Temperature monitoring is essential in friction stir welding (FSW), especially when working with temperature-sensitive alloys like AA3103. In this study, infrared thermography was used as a non-contact method to track real-time thermal

(a) Material Flow Direction for experiment 1 to 9

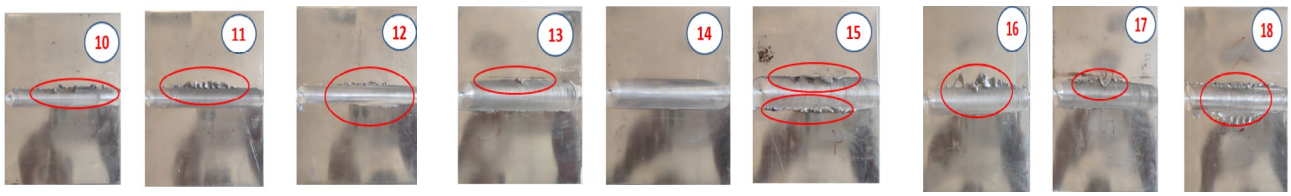

(b) Material Flow Direction for experiment 10 to 18

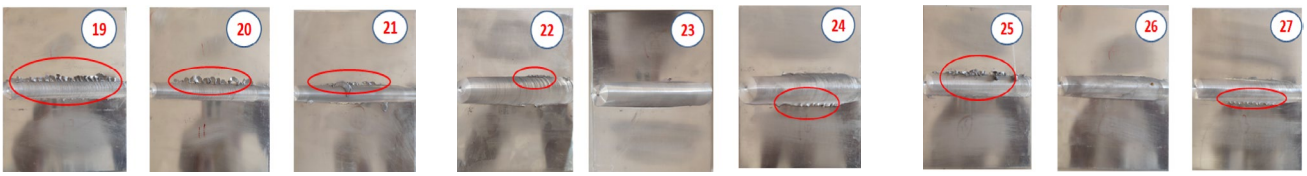

(c) Material Flow Direction for experiment 19 to 27

Fig. 3 Material flow direction for all 27 experiments

Fig. 4 Recording of Temperature using infrared thermometer during friction stir welding

behavior during welding as shown in Fig. 4. Temperature data was captured continuously along the weld path, allowing for analysis of heat input under different process settings. Across all 27 trials, several consistent trends emerged as given in Table 3. Spindle speed was found to have the strongest influence on the peak temperature within the weld zone. When the rotational speed was increased from 355 to 1400 rpm, the maximum temperature rose from about 159 °C to nearly 239 °C, mainly because higher rotation generates greater frictional energy at the tool–material interface. Traverse speed showed the opposite trend. Lower welding speeds, such as 20 mm/min, allowed more time for heat buildup and resulted in higher peak temperatures, around 234 °C. In contrast, increasing the welding speed to 80 mm/min reduced the overall heat input, leading to comparatively lower temperatures. The shoulder-to-pin diameter ratio (D/d) also affected thermal behavior by altering the effective contact area between the tool shoulder and the workpiece. A higher ratio of 5 generated more frictional heat than a ratio of 3 when other parameters were kept constant. Tool pin shape further influenced temperature development. Square

Table 3 Temperature recorded during distance travelled by tool

Exp. no	D/d ratio	Tool profile	Speed of spindle (RPM)	Speed of weld (mm/min)	Temperature recorded during distance travelled by tool (0–150 mm)					
					Initial	30 mm	60 mm	90 mm	120 mm	Tool removal
1	15/5 = 3	Square tool profile	355	20	92	114	132	140	146	151
2	15/5 = 3		710	40	103	125	143	151	157	162
3	15/5 = 3		1400	80	110	132	150	158	164	169
4	20/5 = 4		355	40	116	138	156	164	170	175
5	20/5 = 4		710	80	123	145	163	171	177	182
6	20/5 = 4		1400	20	140	162	180	188	194	199
7	25/5 = 5		355	80	125	147	165	173	179	184
8	25/5 = 5		710	20	140	162	180	188	194	199
9	25/5 = 5		1400	40	174	196	214	222	228	233
10	15/5 = 3	Circular tool profile	355	20	79	101	119	127	133	138
11	15/5 = 3		710	40	97	119	137	145	151	156
12	15/5 = 3		1400	80	99	121	139	147	153	158
13	20/5 = 4		355	40	103	125	143	151	157	162
14	20/5 = 4		710	80	110	132	150	158	164	169
15	20/5 = 4		1400	20	125	147	165	173	179	184
16	25/5 = 5		355	80	121	143	161	169	175	180
17	25/5 = 5		710	20	127	149	167	175	181	186
18	25/5 = 5		1400	40	165	187	205	213	219	224
19	15/5 = 3	Triangular tool profile	355	20	100	122	140	148	154	159
20	15/5 = 3		710	40	113	135	153	161	167	172
21	15/5 = 3		1400	80	124	146	164	172	178	183
22	20/5 = 4		355	40	128	150	168	176	182	187
23	20/5 = 4		710	80	145	167	185	193	199	204
24	20/5 = 4		1400	20	175	197	215	223	229	234
25	25/5 = 5		355	80	144	166	184	192	198	203
26	25/5 = 5		710	20	157	179	197	205	211	216
27	25/5 = 5		1400	40	180	202	220	228	234	239

and threaded pins produced greater heat compared to circular pins, primarily due to stronger mechanical stirring and increased surface interaction with the material. This was confirmed by the temperature vs. distance graphs, which consistently showed higher thermal peaks for square pins. These results highlight that the combination of high spindle speed, large D/d ratio, and low welding speed maximizes heat input leading to improved material plasticization and weld quality. However, excessive heat can lead to undesirable effects like grain coarsening or microstructural degradation, underlining the importance of thermal control in FSW. The Fig. 5a, b, c reinforce the conclusion that tool geometry, along with process parameters, directly governs thermal behavior. These findings are especially relevant for industries requiring high-strength, defect-free welds in aluminium alloys, such as aerospace and automotive sectors.

Surface Roughness Analysis

Surface roughness (Ra) was measured along the weld seam to assess the quality of the welded surface under different FSW process conditions as shown in Fig. 6. In Table 4, the surface roughness values (Ra) showed a wide variation across different parameter combinations. The lowest roughness, about 1.37 µm, was achieved with a square pin tool operating at 710 rpm, a welding speed of 20 mm/min, and a D/d ratio of 4. On the other hand, the highest roughness, approximately 30.85 µm, was recorded at 355 rpm, 80 mm/min, and a D/d ratio of 5, which suggests insufficient heat generation and unstable material flow during welding. Analysis of the roughness data and corresponding plots revealed several clear patterns. Circular pin tools generally produced smoother weld surfaces compared to square and triangular profiles, mainly because of their more consistent and uniform stirring action. Increasing spindle speed tended to enhance surface quality by promoting better heat input and improved plasticization of the material. Similarly, lower traverse speeds supported more effective mixing, resulting in smoother weld beads. In contrast, higher D/d ratios were associated with increased roughness, possibly due to excess heat input and the formation of flash. For example, at 710 rpm and a D/d ratio of 4, raising the welding speed from 20 to 80 mm/min led to a noticeable increase in Ra, from around 1.37 µm to about 9.44 µm. Overall, optimal surface finish was achieved using high spindle speed, low welding speed,

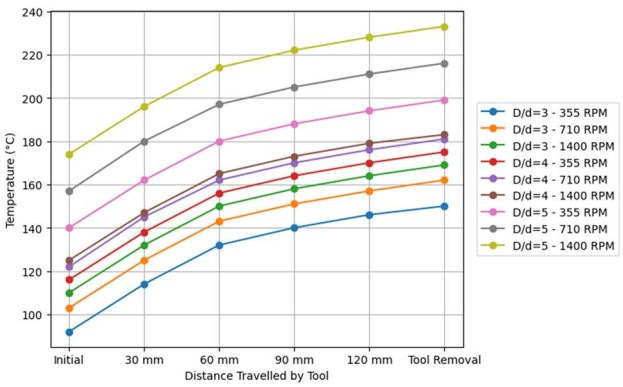

(a) For Square Tool

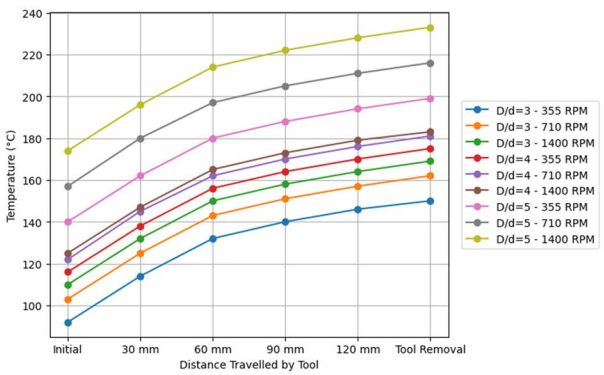

(b) Circular Tool

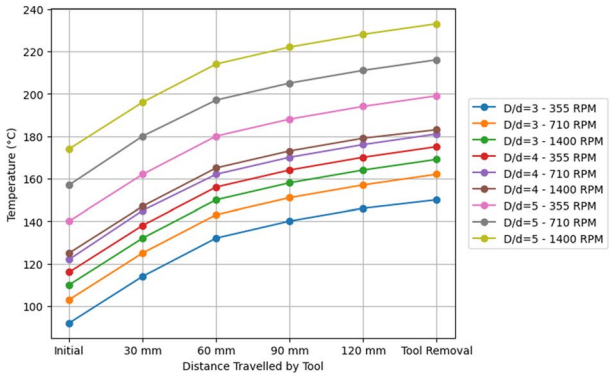

(c) For Triangular Tool

Fig. 5 Temperature distribution graph Vs distance travelled by tool

(a) Mitutoyo On-Site Roughness Measuring Machine

(b) Measurement of roughness of weld using roughness tester for experiment number1

Fig. 6 Roughness measurement

Table 4 Roughness value recorded at different conditions of weld

Square tool profile		Circular tool Profile		Triangular tool Profile	
Exp. no	Welding roughness in µm	Exp. no	welding roughness in µm	Exp. no	welding roughness in µm
1	2.578	10	8.709	19	14.402
2	13.934	11	13.814	20	10.297
3	2.395	12	3.274	21	3.604
4	16.936	13	26.9	22	30.826
5	1.366	14	9.443	23	11.757
6	9.808	15	6.395	24	6.304
7	30.853	16	27.638	25	15.572
8	7.111	17	4.981	26	5.862
9	7.196	18	4.298	27	6.281

and moderate D/d ratios, particularly when combined with circular or square pin profiles. These settings promoted consistent material flow, minimized surface defects, and resulted in smooth, aesthetically acceptable weld beads. The graphical data (Ra line plots, histograms, and scatter plots) reinforce these trends and validate the influence of parameter selection on weld surface morphology.

Histogram of Surface Roughness

In Fig. 7 presents the frequency distribution of surface roughness values obtained from 27 friction stir welding trials, providing insight into the overall surface quality achieved. Most of the experimental samples fall within the 3–10 µm roughness range, indicating that the weld surfaces were generally smooth and within acceptable limits. However, a small number of trials, specifically runs 7, 13, 16, and 22, recorded roughness values above 25 µm. These higher values point to localized surface irregularities caused by less favorable combinations of process parameters. The kernel density estimation curve shows one prominent peak with a long tail extending toward higher roughness values. This pattern indicates a positively skewed distribution, where most welds exhibit low to moderate roughness, while only a few cases display significantly higher surface irregularities. This behavior highlights the strong influence of tool pin profile, rotational speed, and shoulder-to-pin diameter ratio on surface finish, emphasizing the need for optimized parameter selection to ensure consistent and uniform weld quality.

Scatter Plot of Surface Roughness vs Rotational Speed

Figure 8 illustrates the relationship between rotational speed and surface roughness for different tool pin profiles, revealing distinct behavioral trends rather than a clear linear dependence. The square pin profile tends to generate comparatively higher roughness values at medium to higher rotational speeds, which becomes more pronounced when a larger shoulder-to-pin diameter ratio is employed, likely due to excessive material flow and turbulence. In contrast, the circular pin profile maintains relatively uniform and moderate roughness across the speed range, with the most stable response observed around 1400 RPM, indicating improved heat distribution and controlled plastic deformation. The triangular pin profile produces scattered results, alternating between low and high roughness, suggesting that its performance is highly sensitive to changes in processing conditions.

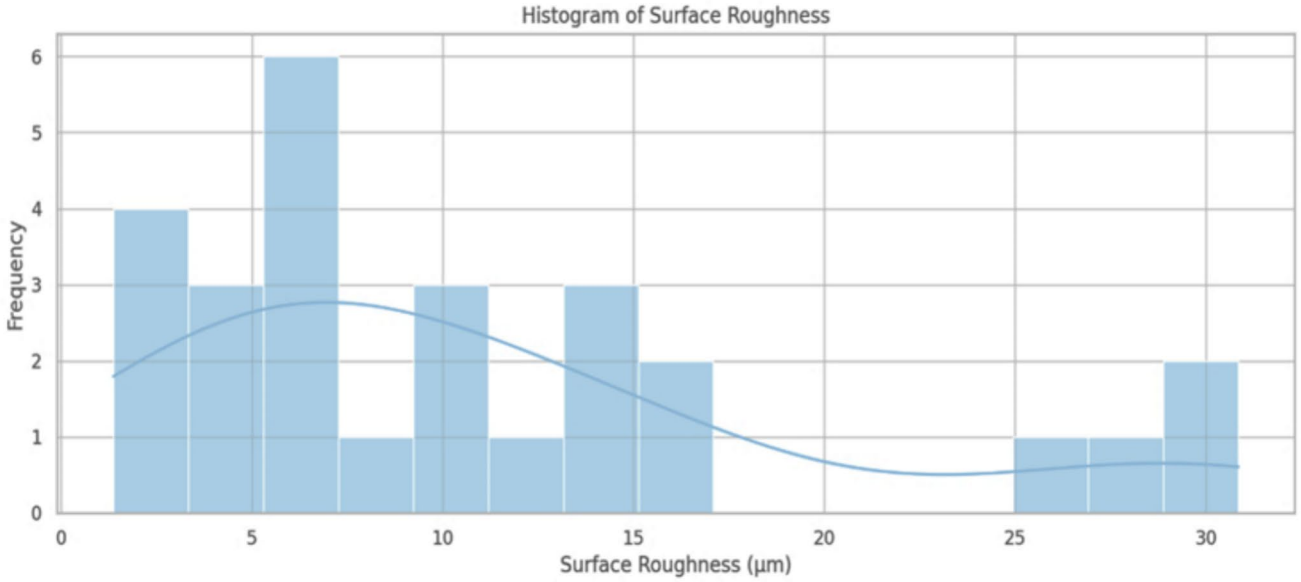

Fig. 7 Histogram of surface roughness

The results indicate a non-linear interaction between tool geometry and processing parameters that significantly influences surface quality. Among the profiles studied, circular pins demonstrate more stable behavior at higher rotational speeds, producing uniform material flow and controlled heat generation. This stability makes circular tools more suitable for achieving consistent and reliable surface finish in AA3103 joints.

Individual Control (I) Chart of Surface Roughness

In Fig. 9 presents the Individuals (I) chart for surface roughness obtained from all 27 friction stir welding experiments, providing an evaluation of process stability. The central line represents the average roughness value of approximately 11.20 µm, while the upper and lower control limits are established at three standard deviations from the mean. Most experimental points lie within these limits, indicating a generally stable process. However, experiments 7, 13, 16, and 22 fall beyond the control boundaries, signifying the presence of special-cause variations. These abnormal deviations are likely associated with unfavorable parameter combinations, particularly excessive shoulder-to-pin diameter ratios and non-optimal welding speeds, which can disrupt material flow and heat input, leading to increased surface irregularities and reduced process consistency.

Although certain parameter combinations produce smooth and repeatable weld surfaces, the I-chart shows noticeable scatter around the mean roughness value. This variability points to inconsistent heat generation and unstable material flow during welding. Such fluctuations indicate that the friction stir welding process for AA3103, under the present operating conditions, has not yet achieved full statistical stability. Therefore, tighter control and optimization of process parameters are essential to ensure reliable surface quality in practical and large-scale industrial application.

3D Surface Plot: Effect of Rotational Speed and Welding Speed on Surface Roughness

Figure 10 illustrates the combined influence of rotational speed and welding speed on surface roughness during friction stir welding of AA3103 through a three-dimensional surface plot. The response surface plot highlights a clear non-linear relationship between rotational speed and welding speed, rather than a straightforward linear trend. Surface roughness rises significantly when high rotational speeds are combined with low welding speeds. This behavior is likely due to excessive heat input, which can disturb material flow and lead to surface irregularities. In contrast, moderate levels of both rotational and welding speeds create a well-defined region of lower roughness. Under these conditions, heat generation and material flow remain balanced, promoting stable plastic deformation and more uniform heat distribution across the weld zone. The accompanying contour projections represent constant roughness levels, enabling clear identification of favorable processing windows. These visual tools assist in selecting practical parameter ranges that promote smoother weld surfaces and improved process reliability in FSW applications.

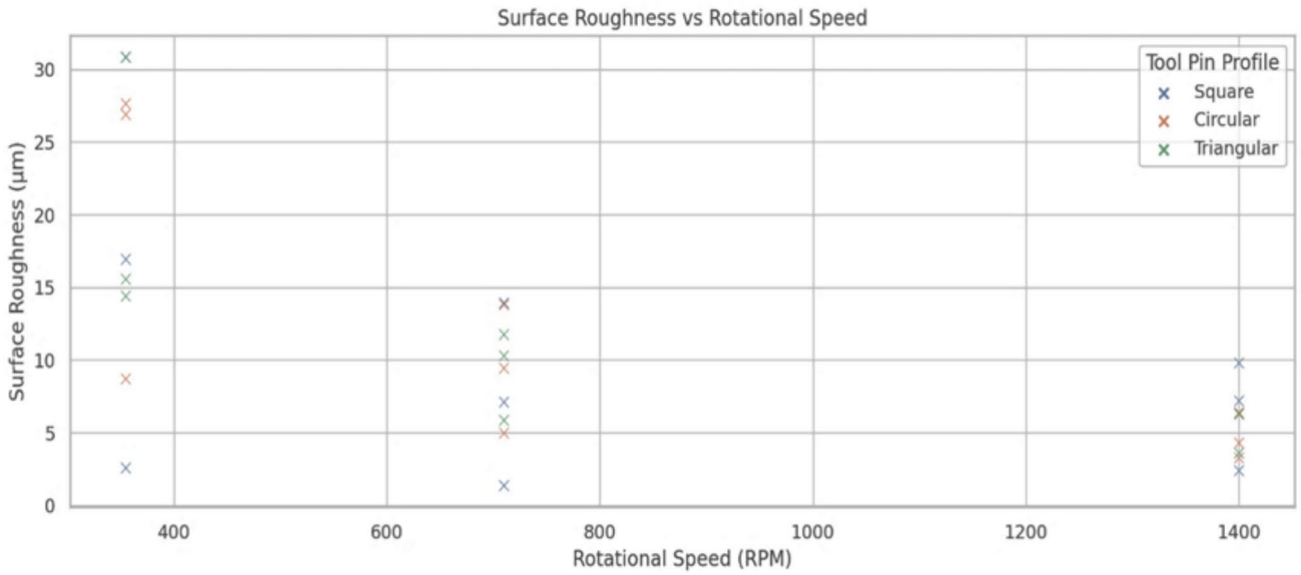

Fig. 8 Scatter plot of surface roughness Vs rotational speed

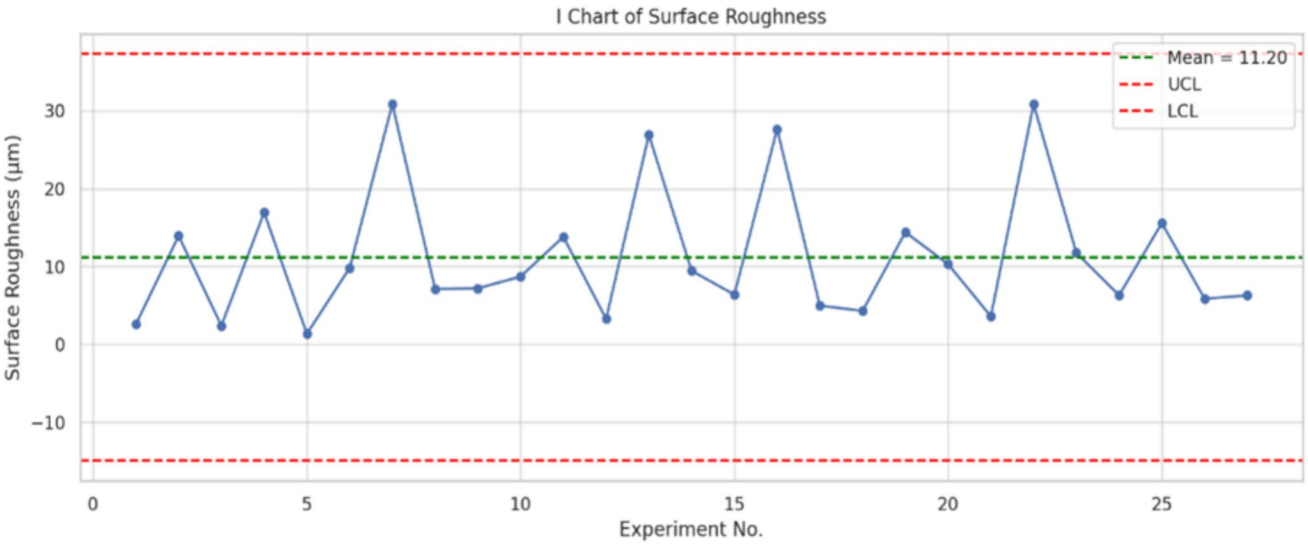

Fig. 9 Individual control (I) chart of surface roughness

Mathematical Modelling

Heat generation (tool → workpiece) Total frictional power input is approximated as the sum of shoulder and pin contributions given in Eq. 1:

$$\dot{Q}_{total} = \dot{Q}_{sh} + \dot{Q}_{pin} \tag{1}$$

For a rotating tool of angular speed, following common FSW approximations given in Eq. 2:

$$\dot{Q}_{\text{sh}} = \int_{r_p}^{r_s} \tau(r)\,\omega\,2\pi r\,dr \quad \text{and} \quad \dot{Q}_{\text{pin}} = \int_{0}^{r_p} \tau_p(r)\,\omega\,2\pi r\,dr \tag{2}$$

If Coulomb friction and uniform shear are assumed, these reduce to closed forms given by Eq. 3:

$$\dot{Q}_{\text{sh}} \approx \frac{2\pi}{3}\,\tau_s\,\omega\left(r_s^3 - r_p^3\right), \qquad \dot{Q}_{\text{pin}} \approx \frac{2\pi}{3}\,\tau_p\,\omega\,r_p^3 \tag{3}$$

where r_s and r_p are shoulder and pin radii, and τ_s, τ_p are effective shear stresses at shoulder and pin surfaces (fit from experiments or taken from literature). The D/d ratio used in the paper relates to r_s/r_p.

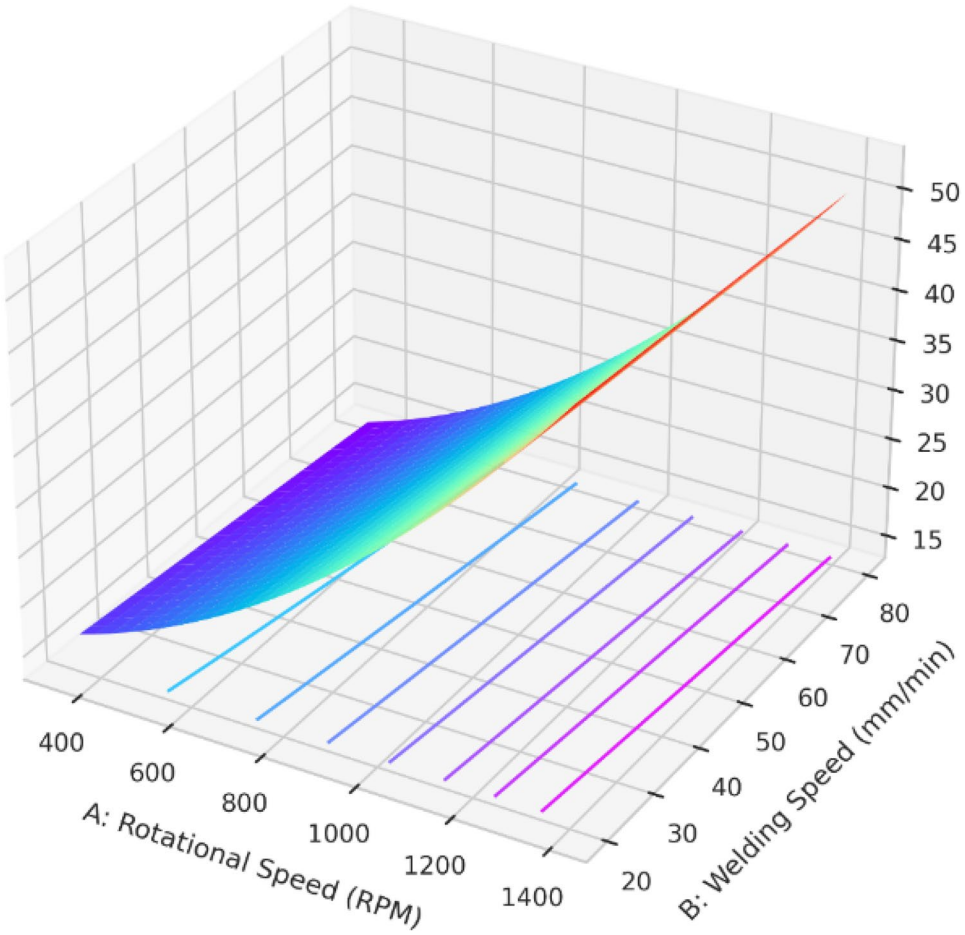

Fig. 10 3D surface plot showing the influence of rotational speed and welding speed on surface roughness

Transient heat conduction (weld zone) Temperature field T(x, t) in the plate satisfies the heat equation with a moving internal heat source represent in Eq. 4:

$$\rho c_p \frac{\partial T}{\partial t} = k\nabla^2 T + \dot{q}(x - Vt) \tag{4}$$

where ρ, c_p, k are density, specific heat and thermal conductivity of AA3103, $\boldsymbol{V}$ is traverse velocity vector (m/s) and $\dot{q}$ is localized volumetric heat input derived from $\dot{Q}_{total}$. For an approximate steady-state along the weld line we may use a moving Gaussian heat source given by Eq. 5:

$$\dot{q}(x, y) = \frac{\dot{Q}_{total}}{2\pi\sigma_x\sigma_y} exp\left(-\frac{x^2}{2\sigma_x^2} - \frac{y^2}{2\sigma_y^2}\right) \tag{5}$$

Boundary conditions: convective cooling at the plate surface by Eq. 6,

$$-k\frac{\partial T}{\partial z}|_{z=0} = h\left(T - T_\infty\right) \tag{6}$$

and initial $T(x, 0) = T_\infty$. Solve numerically (finite element) or use analytical moving-source approximations to estimate peak temperature $T_{\max}$.

Non-dimensional parameters. Define Peclet number to compare advection and diffusion is given by Eq. 7:

$$\mathrm{Pe} = \frac{V\,L}{\alpha}, \qquad \alpha = \frac{k}{\rho c_p} \tag{7}$$

where L is characteristic length (e.g. pin diameter). Higher Pe indicates stronger advective transport (faster traverse → lower heat accumulation).

Empirical model for surface roughness (Ra) Model Ra as a combined effect of process variables: spindle speed N, welding speed V, D/d ratio R, and tool geometry G (categorical). A quadratic response-surface form as given in Eq. 8:

$$\begin{aligned}\mathrm{Ra} = {} & \beta_0 + \beta_1 N + \beta_2 V + \beta_3 R + \beta_4 G_1 + \beta_5 G_2 \\ & + \beta_{11} N^2 + \beta_{22} V^2 + \beta_{33} R^2 + \beta_{12} NV + \beta_{13} NR + \beta_{23} VR + \varepsilon\end{aligned} \tag{8}$$

Tool geometry is encoded with dummy variables G_1, G_2 (e.g. circular = (0,0), square = (1,0), triangular = (0,1)).

Coefficients β are estimated by ordinary least squares using the 27 measured Ra values. Model adequacy is checked via R^2, residual analysis and ANOVA; interactions retained only if statistically significant ($p < 0.05$).

Taguchi/S/N treatment (smaller-the-better for Ra) Signal-to-Noise ratio used in Taguchi analysis for minimization as given in Eq. 9:

$$\mathrm{S/N} = -10\log_{10}\left(\frac{1}{n}\sum_{i=1}^{n} y_i^2\right) \tag{9}$$

where y_i are replicate Ra measurements (use single measurement per run here). Use S/N means to rank factor levels and confirm with ANOVA to compute percentage contribution as given by Eq. 10:

$$\mathrm{Contributionn}_{\mathrm{factor}} = \frac{\mathrm{SS}_{\mathrm{factor}}}{\mathrm{SS}_{\mathrm{total}}} \times 100\% \tag{10}$$

(SS = sum of squares).

Linking thermal model and Ra (phenomenological relation). A compact predictive relation (to be verified by regression) linking peak temperature and Ra in Eq. 11:

$$\mathrm{Ra} = a_0 + a_1 T_{max}^{-1} + a_2 V + a_3 R + a_4 G + \eta \tag{11}$$

reflecting that higher $T_{\max}$(better plasticization) generally reduces Ra. Fit coefficients a_i from experimental $T_{\max}$ and Ra pairs, evaluate significance and predictive error.

A total of 27 friction stir welding trials were conducted on AA3103 aluminium alloy using three distinct tool pin profiles, namely square, circular, and triangular, under Taguchi L9 design conditions. The experimental analysis revealed that spindle speed was the most significant parameter affecting weld quality, contributing nearly half of the overall variation, followed by the shoulder-to-pin diameter ratio and tool geometry. Material flow observations confirmed that circular pins produced more stable and uniform welds, whereas square pins induced stronger stirring but occasionally led to flash and surface defects at high shoulder-to-pin ratios.

Temperature distribution was found to increase with spindle speed and D/d ratio, while slower welding speeds allowed greater heat input. The maximum peak temperature of about 239 °C was recorded at 1400 RPM with D/d = 5. Surface roughness analysis indicated that the smoothest weld, with an Ra value of about 1.37 µm, occurred at 710 RPM, 20 mm/min, and D/d = 4 using the square pin, while the roughest surface, measuring nearly 30.8 µm, was observed at 355 RPM, 80 mm/min, and D/d = 5. Circular pins consistently produced smoother weld surfaces across a wider range of parameters, confirming their suitability for surface-sensitive applications. The mathematical modelling of heat generation, transient heat transfer, and surface roughness prediction showed good agreement with experimental results, validating the combined use of Taguchi design of experiments and phenomenological modelling. Statistical analysis, including ANOVA and signal-to-noise ratio, confirmed that high spindle speeds, low traverse speeds, and moderate D/d ratios provided the best balance between heat input, plasticization, and surface finish.

Conclusion

This work carried out a comprehensive Taguchi-based experimental study on friction stir welding of AA3103 aluminium alloy by combining thermal observation, surface finish assessment, and predictive modelling. Unlike earlier investigations that largely concentrated on high-strength aluminium grades such as AA6061 and AA7075, the present study emphasizes AA3103, a corrosion-resistant alloy widely used in industrial applications. The experimental outcomes revealed that rotational speed plays the most significant role in determining weld quality, followed by the shoulder-to-pin diameter ratio and the geometry of the tool pin. Among the profiles examined, circular pins produced smoother surfaces owing to more uniform material flow, whereas square pins generated higher heat input and stronger stirring action, leading to finer yet less consistent weld characteristics. An optimal parameter set consisting of a spindle speed of 710 RPM, a traverse speed of 20 mm/min, and a D/d ratio of 4 resulted in sound, defect-free joints with minimal surface roughness. The originality of this study stems from the integrated use of Taguchi experimental design, infrared thermal analysis, and surface roughness modelling specifically for AA3103 alloy. The conclusions provide both optimized process guidelines and a transferable methodological approach applicable to other aluminium alloys. Further research should explore post-weld heat treatments, microstructural evolution, and tool durability during extended welding cycles to improve industrial implementation.

Funding This review did not receive any specific grant from funding agencies in the public, commercial, or not-for-profit sectors.

Data Availability The data that support the findings of this study are available from the corresponding author upon reasonable request.

Declarations

Conflict of interest The authors declare that they have no known competing financial interests or personal relationships that could have appeared to influence the work reported in this paper.

References

1. M.M.Z. Ahmed, A.R.S. Essa, S. Ataya, M.M.E. Seleman, A. Abd El-Aty, B. Alzahrani, K. Touileb, A. Bakkar, J.J. Ponnore, A.Y.A. Mohamed, Friction stir welding of AA5754-H24: impact of tool pin eccentricity and welding speed on grain structure, crystallographic texture, and mechanical properties. Materials **16**(5), 2031 (2023)
2. M.M.Z. Ahmed, M.M. El-Sayed Seleman, D. Fydrych, G. Çam, Friction stir welding of aluminium in the aerospace industry: the current progress and state-of-the-art review. Materials **16**(8), 2971 (2023)
3. O.P. Abolusoro, E.T. Akinlabi, Effects of processing parameters on mechanical, material flow and wear behaviour of friction stir welded 6101-T6 and 7075-T651 aluminium alloys. Manuf. Rev. **7**, 1 (2020)
4. A. Alavi Nia, R. Amirifar, Experimental study of the effects of pin geometry, advancing speed and D/d ratio on the mechanical and microstructural properties of 6061 aluminium alloy under the friction stir processing. J. Adv. Join. Process. **9**, 100205 (2024)
5. A. Amin, G. Hussain, Detection of friction stir welding defects of AA1060 aluminium alloy using specific damping capacity. Metals **8**(4), 337 (2018)
6. A. Belaziz, M. Bouamama, I. Elmeguenni, S. Zahaf, Experimental study of the roughness variation of friction stir welding FSW. Mater. Phys. Mech. **51**(3), 115–125 (2023)
7. A. Chakkravarthi, V. Kumar, G. Phanikumar, C. Murugesan, Experimental investigation of friction stir welding on 6061-T6 aluminium alloy using Taguchi-based grey relational analysis. Metals **10**(11), 1480 (2019)
8. M.S. Chander, M. Ramakrishna, B. Durga Prasad, A. Rajesh, A review on impact of tool pin geometry on friction stir welding of aluminium alloys. IOP Conf. Ser. Mater. Sci. Eng. **981**, 042018 (2020)
9. A.R.S. Essa, A.R.K. Aboud, M.M.Z. Ahmed, A.E. El-Nikhaily, A.S. Easa, M.I.A. Habba, Friction stir welding of aluminium alloy 6082-T6 using eccentric shoulder tools to eliminate the need for tool tilting. Sci. Rep. **15**(1), 8801 (2025)
10. I. Feddal, M. Chairi, G. DiBella, Analysis of friction stir welding of aluminium alloys. Metals **15**(5), 532 (2025)
11. A.S. Hammad, H.T. Lữ, M.M.E. Seleman, M.M.Z. Ahmed, A. Alamry, J. Zhang, H. Huang, B. Alzahrani, G. Yang, A. Abd El-Aty, I.S. El-Deeb, Impact of the tool shoulder diameter to pin diameter ratio and welding speed on the performance of friction stir-welded AA7075-T651 Al alloy butt joints. Mater. Res. Express **11**(5), 056506 (2024)
12. W.H. Khalafe, L.S. Ewe, M.R.B. Isa, A.B. Omran, S.B. Shamsudin, The effect of friction stir welding parameters on the weldability of Aluminium alloys with similar and dissimilar metals: review. Metals **12**(12), 2099 (2022)
13. H. Khazal, A. Belaziz, R. Al-Sabur, H.I. Khalaf, Z. Abdelwahab, Unveiling surface roughness trends and mechanical properties in friction stir welded similar alloys joints using adaptive thresholding and grayscale histogram analysis. J. Manuf. Mater. Process. **9**(5), 159 (2025)
14. V. Lunetto, M. De Maddis, F. Lombardi, P. Russo Spena, A review of friction stir welding of industrial alloys: tool design and process parameters. J. Manuf. Mater. Process. **9**(2), 36 (2025)
15. R.D. Nazarlou, S. Salim, M. Wiegand, C. Wolf, S. Böhm, Mechanical and microstructural properties of high-speed friction stir welding of AA7020 Aluminium alloy using multi-pin tool. Metals **15**(5), 511 (2025)
16. M.H. Osman, N.F. Tamin, Influence of tool pin profile on the mechanical strength and surface roughness of AA6061-T6 overlap joint friction stir welding. J. Mech. Eng. Sci. **17**(3), 0758 (2023)
17. G. Patsalias, K. Sofias, A. Vairis, Solid-state welding of thin aluminium sheets: a case study of friction stir welding alloys 1050 and 5754. Metals **15**(4), 463 (2025)
18. M.M. Math, R. Sridhar, A. Bharatish et al., Mechanical characteristics of SLA printed parts using photopolymer resin. J. Inst. Eng. (India): Ser. D (2025). https://doi.org/10.1007/s40033-025-00954-2
19. M. Vinod, C.A. Kumar, S.B. Sollapur et al., Study on low-velocity impact performance of chemical treated flax fibre-reinforced aluminium 6082 laminates. J. Inst. Eng. India Ser. D. (2024). https://doi.org/10.1007/s40033-024-00657-0
20. M. Kolli, C. Sunnapu, N.R. Medikondu, Multi-response optimization of friction stir welding process parameter of AA 5083 with Taguchi-VIKOR approach. J. Eng. Appl. Sci. **72**(1), 2 (2025). https://doi.org/10.1186/s44147-024-00572-x
21. S.B. Sollapur, R.K. Mantri, D. Baviskar, Y.A. Kharche, S.R. Shekokar, Influence of fillers on high-temperature tribology of metal matrix composites. in *Micro-and Nanocomposites*, (CRC Press), pp. 121–136
22. K. Wang, A. Naumov, E. Panchenko, O. Panchenko, A review on friction stir welding of high-strength Al-Zn-Mg alloy: insights on second-phase particles. Materials **17**(20), 5107 (2024)
23. D. Saravanan et al., Tribological properties of filler and green filler reinforced polymer composites. Mater. Today Proc. **50**, 2065–2072 (2022). https://doi.org/10.1016/j.matpr.2021.09.414
24. M. Vinod, C.A. Kumar, S.B. Sollapur et al., Study on fabrication and mechanical performance of flax fibre-reinforced aluminium 6082 laminates. J. Inst. Eng. India Ser. D (2023). https://doi.org/10.1007/s40033-023-00605-4
25. C. Nagaraj, K.M. Dutt, G.K. Manjunath et al., Effect of multidirectional forging on grain structure and mechanical properties of hypereutectic Al–20% Si alloys with added refiners and modifiers. Can Metall Quarterly **64**(3), 969–983 (2025). https://doi.org/10.1080/00084433.2024.2413245
26. S.B. Sollapur, P.C. Sharath, B.R. Bharathkumar, K. Hemanth, B.R Vishwanath, A.K. Hosamani, Influence of micro-sized filler reinforcement in tribological performance of ceramic matrix composites. in *Micro-and Nanocomposites*, (CRC Press), pp. 197–216
27. S. Yang, S. Chen, H. Song, J. Shen, Effects of tool geometry on the weld quality of friction stir welded ultra-thin 1060 aluminium alloy plate. Int. J. Light. Mater. Manuf. (2025). https://doi.org/10.1016/j.ijlmm.2025.06.001